INVESTIGATION OF CLOUD PROPERTIES AND ATMOSPHERIC STABILITY WITH MODIS

SEMI-ANNUAL REPORT FOR JAN - JUN 1992

Paul Menzel
NOAA/NESDIS at the University of Wisconsin

Contract NAS5-31367

TASK OBJECTIVES

Reconfigure MAS. The MAS (MODIS Airborne Simulator) will be reconfigured to its full capability (including longwave C02 channels) for cloud investigations in August and engineering checkout will proceed in November. UW will assist in the instrument evaluation to confirm stable performance for TOGA-COARE.

Algorithm Definition. Using the MAS/FIRE data from Nov-Dec 1991, investigate the algorithms for specifying cloud parameters. Determine the appropriate adjustments for signal noise, spatial resolution, and temporal resolution. Study situations of single layer thin cloud, mixed layers of ice and water cloud , over land, over ocean. From the MAS investigations, infer the best MODIS algorithms within the next year.

MODIS Instrument Review. The calibration and spectral selection of the MODIS infrared channels will continue to demand attention. Simulations of the impact of spectral channel changes on the cloud parameter derivation should continue to guide instrument developers.

WORK ACCOMPLISHED

MAS Instrument Performance Evaluation. Several test flights of the MAS were evaluated jointly by UW, GSFC and Ames to assess instrument performance. Noise in the six thermal channels (3.75, 4.5, 4.65, 8.8, 10.95, 11.95 microns) was found to be .5 to 1.5 C over uniform scene in the Gulf of Mexico (rms was 1.7, 0.6, 0.8, 0.3, 0.4, 0.7 C respectively). Calibration with an ice bucket revealed biases from .1 to 1.3 C (measured minus truth were 1.0, 1.3, 1.3, .7, .1, .4 C respectively without benefit of complete spectral response data or correction for residual atmospheric absorption); this was considered to be quite good raising confidence in inflight calibration. However it was determined that to reduce the effects of single sample noise in the calibration (which reveals itself as striping in the image), the blackbody counts of the MAS must be smoothed for several scan lines (eg. nine lines). Inflight gain (radiance per count) changes of 10 to 20% were recorded as the instrument temperature dropped from 240 K to 230 K inflight; this made dynamic range adjustments somewhat hit or miss (further investigation revealed that this was due to thermal expansion/contraction of exterior optics components which could be minimized by heating the dewar exterior). Overall the instrument performance during FIRE in Nov-Dec 1991 was judged to be excellent, given the short amount of preparation time; this is reported in a MAS/FIRE Quick Look Engineering Report prepared by GSFC and UW.

MAS FIRE Flights and Data Processing. Thirteen MAS flights from 12 Nov to 6 Dec during FIRE were flown; these are cataloged in a data book that includes

flight tracks, pilot debriefings, MAS settings, radiometric gains, and noise evaluation. Code for loading, calibrating, and displaying MAS data on McIDAS were written; the capability for qualitative and quantitative analysis of MAS data was established. Processing and screening of MAS data is proceeding at UW; segments from six of the flights were evaluated for cloud situation and data quality on the McIDAS. The data from 16 Nov, 24 Nov, 25 Nov, 26 Nov, and 5 Dec have been selected for initial investigations (the 5 Dec flight over Coffeyville, Kansas has varying thin cirrus over the ground network, 24-26 Nov data show mixed ice and water clouds, and the 16 Nov test is being used to characterize the calibration accuracy). A transmittance regression model has been developed for the infrared spectral channels of the MAS; this model has been used to simulate atmospheric transmittances for MAS channels using radiosondes data.

MAS Reconfiguration. The MAS was reconfigured to its full capability for cloud investigations in April (including the longwave C02 channels). In May, UW took part in the engineering checkout at Ames Research Center, CA. MAS data was collected under cold chamber conditions, room temperature conditions, and in the aircraft hanger using an ice bucket scene for absolute calibration testing. Evaluations of MAS calibration stability in varying ambient conditions , image quality, channel noise and truncation error, 10 bit data, and absolute calibration were performed. Subsequent test flight data was evaluated. Performance was satisfactory for all channels except the 13 micron channels which display strong 400 Hz noise (believed to be from the heaters) and calibration instability; the noise equivalent radiances were about 1.4 and 2.2 C (for a 300 K target) in the 13.3 and 13.9 micron channels respectively. For ASTEX this situation was left unchanged; work will proceed on further modification out to 14.2 microns and improved signal to noise performance in late summer 1992. Test flights in Nov-Dec 1992 will indicate the capability of MAS to achieve clean signals in the 13-14.5 micron range. MAS flights during TOGA-COARE are planned with onsite support at Townsville, Australia by UW and GSFC for six weeks in Jan-Feb 1993.

Thin Cirrus Algorithm Development. Detection of thin ice cirrus with the 8.6, 11 and 12 micron channels of MAS for different cloud regimes was demonstrated with data from the FIRE flights of 24-26 Nov and 5 Dec. Single sample noise necessitated averaging to about 250 meter resolution (25 fields of view). Scatter plots of brightness temperature differences of the 8-11 micron versus 11-12 micron MAS channels indicate differentiation between thick and thin cirrus, low water cloud, and clear sky conditions. A distinct spectral signal emerges for optically thick ice cloud over water which is related to the cloud particle size and cloud emissivity. Initial difficulties in resolving mid level water cloud have been resolved through the assumption that as water clouds become increasingly uniform (eg. from scattered to overcast) the brightness temperatures differences tend to zero. Use of the 11 micron brightness temperature in tandem with the three channel differencing has been constructive in identifying mixed layer cloud that is not obvious from brightness temperature differencing alone. The development of software to sort pixel values in terms of FOV uniformity has begun as a means of determining the effects of varying cloud scenes on the brightness temperature differencing technique.

Shortwave C02 Investigations. Shortwave C02 slicing cloud parameter investigations continued. Shortwave versus longwave skill for height and

emissivity determination were analyzed with three nighttime HIRS data sets; it was found that the shortwave has more skill in defining clouds below 500 mb than the longwave. Different noise characteristics and increased sensitivity to surface radiances are the probable reasons. Definition of an algorithm combining the shortwave and longwave C02 calculations has begun; shortwave will be used as a supplement to the longwave at night. A report is in preparation.

DATA ANALYSIS/INTERPRETATION

Thin Cirrus Algorithm Development with FIRE Data. The following paragraphs present a brief summary of the theory and some of thin cirrus analysis using MAS data (which has been summarized in the previous section of this report),

The absorption of infrared radiation in water and ice clouds shows a distinct separation at wavelengths greater than 10 microns (Figure 1). The maximum difference in ice/water single scattering properties occur at 12 micron; furthermore the slope of the absorption versus wavelength curve is steeper for water than for ice between 11 and 12 microns. This suggests that liquid water clouds will produce a larger brightness temperature difference betweeen 11 and 12 microns than between 8 and 11 microns; ice clouds will cluster in a steeper slope than liquid water clouds in a plot of 8-11 micron versus 11-12 micron brightness temperatures. The essence of the thin cirrus algorithm is to distinguish cloud phase from this property.

Figure 2 shows the scatter plot of MAS brightness temperature differences (8-11 and 11-12) over cirrus (ice) and water cloud from different portions of the MAS flight of 5 Dec 1992. The cirrus cloud stands out as the cluster of points in a line with a slope greater than one and a maximum 8-11 micron value of 4 K. The water cloud is a group of points aligned in a slope less than one . The two cloud types are readily distinguished on the same scatter diagram.

A thick convective cirrus cloud over the Gulf was also investigated using the MAS tri-spectral data. This data was categorized into 15 K intervals of 11 micron brightness temperature, as a means of identifying the location of the scatter points as they relate to the image (Figure 3). A coherent pattern of values is evident. The cloud free region is evident as the warmest brightness temperatures (290-305 K) which cluster with the lowest 8-11 micron brightness temperature differences (0 to -1 K). As the 11 micron brightness temperature decreases, the points cluster with a slope greater than one, representative of ice cloud, peaking at an 8-11 micron brightness temperature value of 4 K. Going to colder brightness temperature values in the center of the cloud, the brightness temperature scatter plot curves toward zero temperature differences. Inoue (1987; 'Journal of geophysical Research, Vol. 92, pages 3991-4000) noted that this is indicative of a black cloud, where each of these "window" channels sense the cold cloud tops at the same temperature. From this simple scatter diagram, clear regions, cloud phase, relative cloud height, and relative cloud emissivity can be determined.

So far, these examples have shown single cloud types and single cloud layers. Multi-layer, multi-phase clouds were also examined from the 5 Dec 1991 flight track. Cloud types range from thick ice cloud, thin ice cloud, water cloud,

and multi-phase cloud. To further differentiate multi-phase cloud, both brightness temperature differences (8-11 and 11-12) were plotted versus the 11 micron brightness temperature (Figure 4 where the dark curves are the 8-11 micron brightness temperature differences and the gray curves are the 11-12 micron differences). Track E is the black ice cloud where the differences eventually go to zero with decreasing brightness temperatures; the 8-11 micron brightness temperature differences are greater than the 11-12 micron differences. Track A is the thin cirrus scene and the 11 micron brightness temperatures are much higher than for the black ice cloud of Track E; the lower emissivity of the cloud prevents it from being detected as a black cloud. The water cloud scene, track D, covers a much smaller 11 micron brightness temperature range and the 11-12 micron brightness temperature differences are much greater than the 8-11 micron differences; the arch in the scatter diagram again shows the points peaking and then curving back toward zero brightness temperature differences, as the 11 micron temperature decreases. Inoue (1987) described this phenomenon as low level black clouds, physically due to the fact that the majority of water vapor lies below these clouds . As the scattered to broken low level cloud layer becomes overcast, less water vapor below cloud level can be detected and the brightness temperature differences go to zero. This suggests that FOV uniformity is another feature that may be detected using the 8, 11 and 12 micron channels. The final panel, track B, is the multi-cloud scene where the patterns from the other three panels are all evident; in addition thin cirrus cloud over low water cloud can be discerned from the arch of points from the low overcast black water cloud (around 270 K) extending into the cirrus arch, combining with it around 255 K. Use of this scatter diagram then, in tandem with the 8-11 versus the 11-12 micron brightness temperature difference scatter diagram, have the potential to differentiate multi-layer and multi-phase clouds.

Investigating Shortwave C02 Slicing with HIRS Data. The following paragraphs present a brief summary of the shortwave C02 slicing algorithm and some comparisons of longwave and shortwave C02 slicing results using HIRS nighttime data (which has been summarized in the previous section of this report).

The HIRS radiometer senses infrared radiation in eighteen spectral bands that lie between 3.9 and 15 microns at 25 to 40 km resolution (depending upon viewing angle) in addition to visible reflections at the same resolution. The four channels in the $C0_2$ absorption band at 4 microns (rather than at 15 microns) are used to differentiate cloud altitudes and the shortwave infrared window channel (rather than the longwave) identifies the effective emissivity of the cloud in the HIRS field of view (FOV). The algorithm is presented in some detail in Menzel et al. (1992).

To assign a cloud top pressure to a given cloud element, the ratio in two spectral bands of the deviations in cloud produced radiances and the corresponding clear air radiances (referred to as cloud forcing) is measured with the HIRS and calculated from a model guess. The measured cloud forcing comes from the HIRS observed radiance in a given fov and the inferred clear air radiance after spatial analyses of neighboring clear radiance observations. The calculated cloud forcing is accomplished with the infrared radiative transfer equation (using NMC model guess temperature profile and the profiles of atmospheric transmittance for the spectral channels) for clouds at different pressure levels. The cloud emissivity is assumed to be the same for

the two spectrally close channels. The cloud pressure that best matches observed and calculated ratios is the desired solution.

The effective cloud amount (fraction times emissivity) is then the ratio of the observed cloud forcing and the cloud forcing of an opaque cloud at the determined cloud pressure.

Using the ratios of radiances of the three C02 spectral channels, four separate cloud top pressures can be determined (4.40/4.46, 4.40/4.52, 4.46/4.52, and 4.52/4.57). Whenever the cloud forcing is within the noise response of the instrument (roughly .01 mW/m2/ster/cm-1), the resulting pressure is rejected. Using the infrared window and the four cloud top pressures, as many as four effective cloud amount determinations can also be made where the cloud height and amount that best satisfy the radiative transfer equation for the four CO_2 channels is chosen.

Figure 5 shows the comparison of the cloud top pressures determined with longwave and shortwave C02 slicing for three HIRS nighttime data sets (this precludes problems with reflected solar radiation in the shortwave channels). Mean differences in the heights are less than 100 mb. Figure 6 shows that the uncertainty in the cloud top pressure determination due to instrument noise is less than 50 mb for both longwave and shortwave; the shortwave C02 slicing algorithm shows more skill in determining mid level cloud top pressures probably due to its better signal to noise. Figure 7 shows the comparison of shortwave and longwave effective emissivities; mean differences are less than 10%. It is apparent from these preliminary results that the two algorithms complement each other; a combined algorithm is suggested.

ANTICIPATED FUTURE ACTIONS

Algorithm Definition. An initial version of the operational MODIS cloud parameter code will be drafted and documentation will be contemplated.

MAS/HIS Intercomparisons. The collocated HIS (High resolution Interferometer Sounder) data will be used for intercalibration of the two instruments (MAS and HIS) and for studying the spectral sensitivity of the cloud parameter algorithms.

Investigating C02 Slicing in Two Cloud Layers. Radiative transfer models will be used to model radiances observed in situations of two cloud layers. The C02 slicing algorithm will be generalized to accommodate both single and multiple cloud layers.

Cloud Investigations with MAS during TOGE-COARE. UW and GSFC members of the Atmospheres Group will be supporting MAS flights out of Townsville, Australia for six weeks in Jan and Feb 1993 as part of TOGA-COARE (Tropical Ocean Global Atmosphere/Coupled Ocean-Atmosphere Response Experiment). Checkout flights will be supported in Nov-Dec 1992 to prepare for TOGA-COARE and to verify good longwave infrared channel performance.

PROBLEMS/CORRECTIVE ACTIONS

We have not yet established access to the MODIS Team Members data base that includes spectral response information (from John Barker) and the day one products files (from Al Fleig). Efforts are underway to plug into these data bases. Eletronic telemail reporting has not been a problem. Otherwise, all seems to be going fine.

PUBLICATIONS

King, M. D., Y. J. Kaufman, W. P. Menzel, and D. Tanre, 1992: Remote Sensing of Cloud, Aerosol and Water Vapor Properties from the Moderate Resolution Imaging Spectrometer (MODIS). IEEE Trans. and Geoscience and Remote Sensing, 30, 2-27.

Menzel, W. P., D. P. Wylie, and K. 1. Strabala, 1992: Seasonal and Diurnal Changes in Cirrus Clouds as seen in Four Years of Observations with the VAS. J. Appl. Meteor. , Vol. 31, No. 4, 370-385.

Strabala, K. I., 1991: Optimum Radiometric Spectral Intervals For Cirrus Detection. Masters Thesis at the University of Wisconsin.

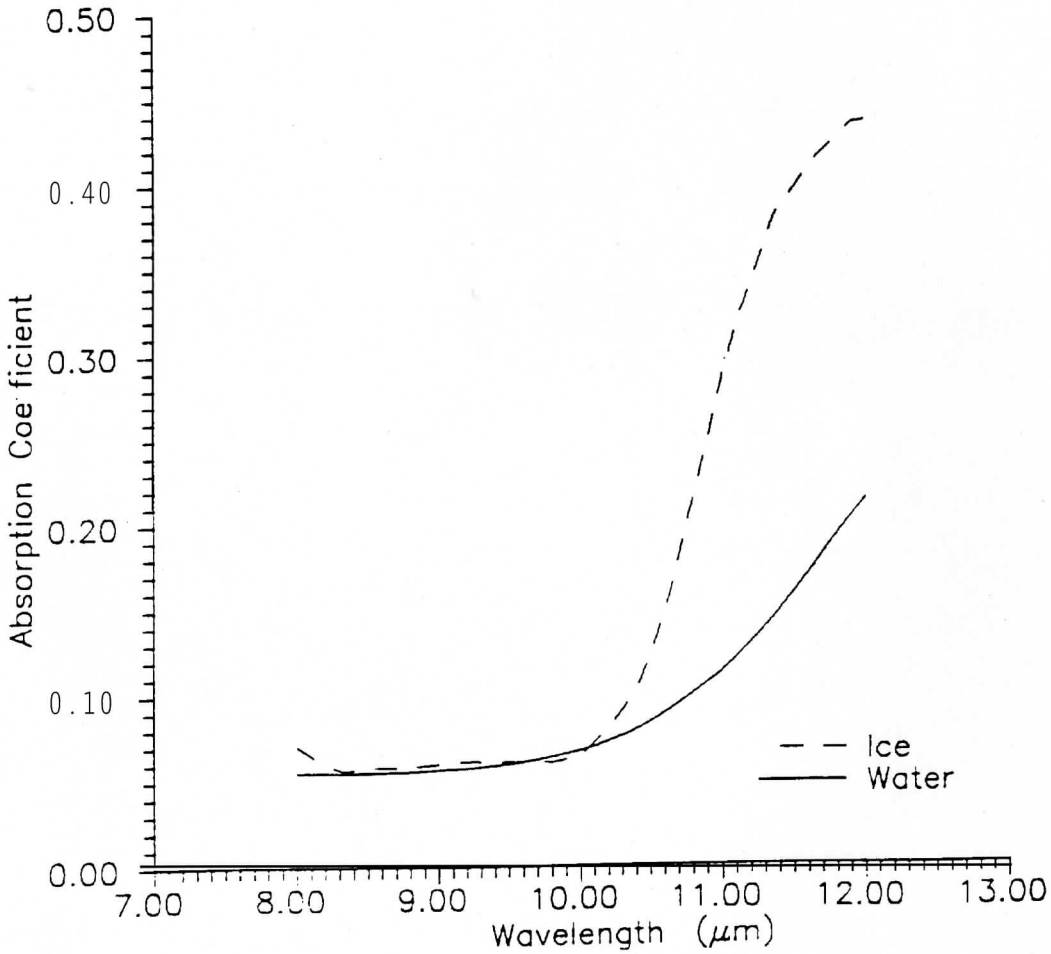
0.50
0.40
0.30
0.20
0.10
0.00
Absorption Coe ficient
7.00
8.00
9.00
10.00
11.00
12.00
13.00
Wavelength (μm)
Ice
Water

Figure 1

CASE A - THIN ICE CLOUD
MAS BAND 11

CASE B - WATER CLOUD
MAS BAND 11

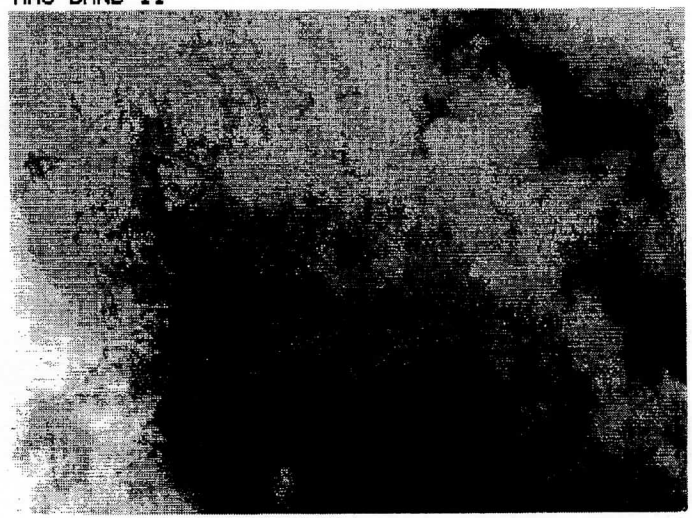

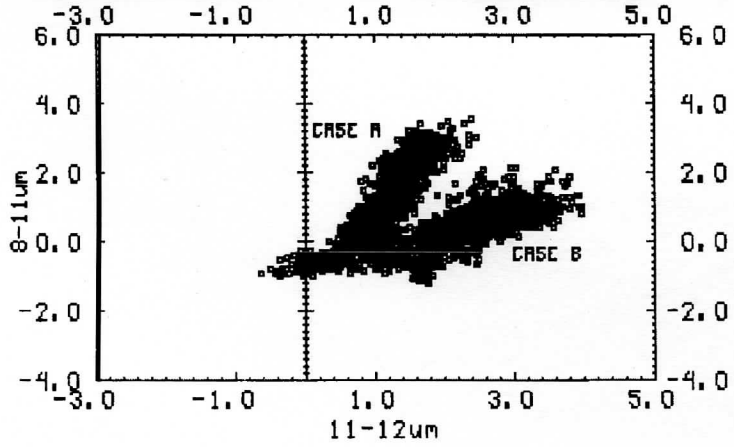

SPECTRAL SiGNATURE OF CLOUD PROPERTIES

AS DETERMINED BY
BRIGHTNESS TEMPERATURE DIFFERENCING
OF THE MODIS AIRBORNE SIMULATOR
INFRARED CHANNELS

MAS FLIGHT
5 DECEMBER 1991

Figure 2

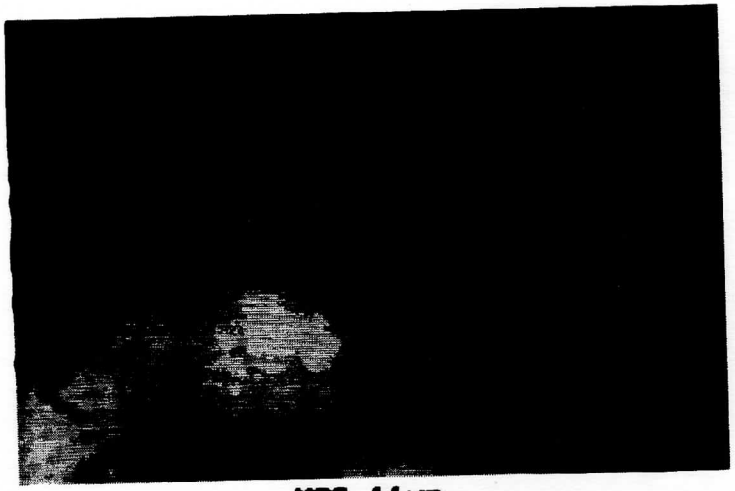

MAS 11um

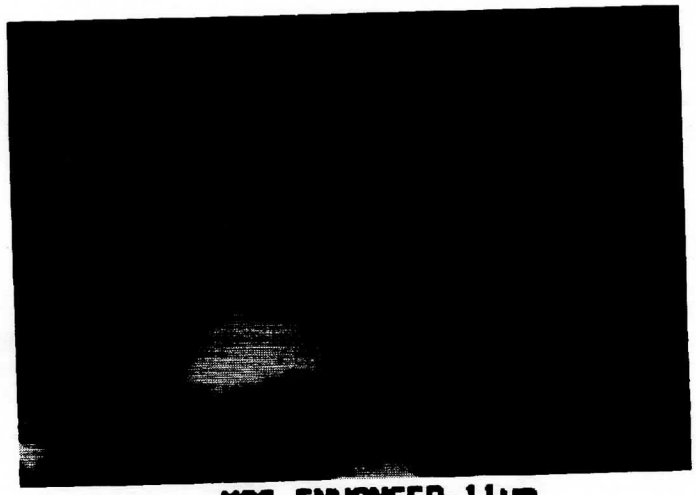

MAS ENHANCED 11um

BRIGHTNESS TEMPERATURE DIFFERENCES

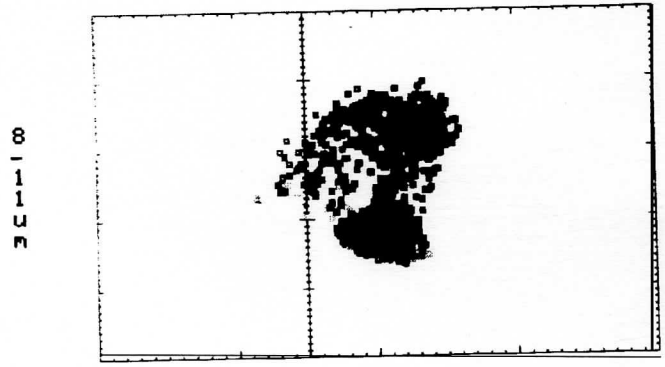

11-12um

SPECTRAL CLOUD SIGNATURES

11um BRIGHTNESS TEMP.

- 215 - 230K
- 230 - 245K
- 245 - 260K
- 260 - 275K
- 275 - 290K
- 290 - 305K

MAS FLIGHT 5 DEC 1991
TRACK E

Figure 3

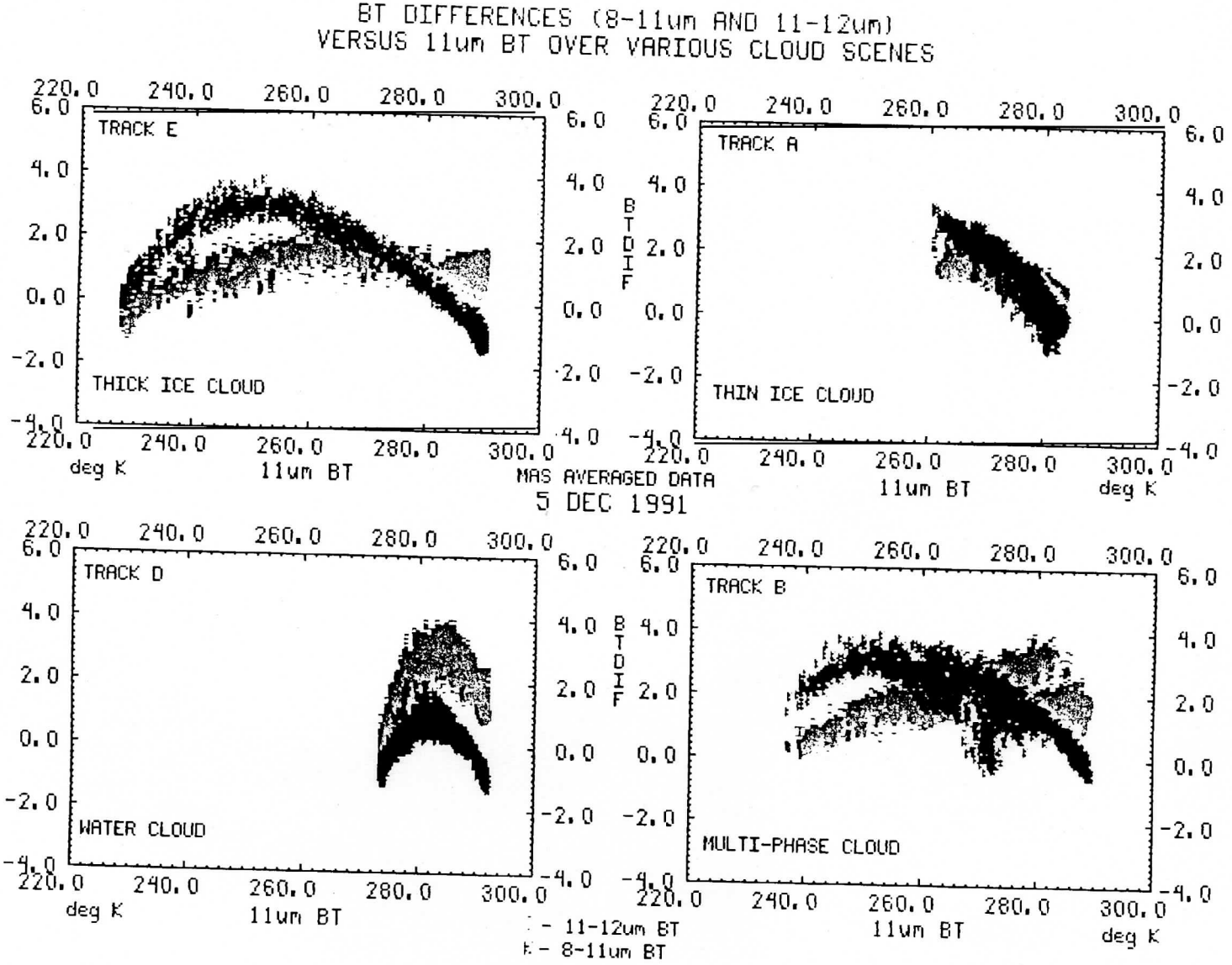
BT DIFFERENCES (8-11um AND 11-12um)
VERSUS 11um BT OVER VARIOUS CLOUD SCENES
TRACK E
THICK ICE CLOUD
TRACK A
THIN ICE CLOUD
TRACK D
WATER CLOUD
TRACK B
MULTI-PHASE CLOUD
BTDIF
deg K
11um BT
MAS AVERAGED DATA
5 DEC 1991
- 11-12um BT
- 8-11um BT

Figure 4

Fig 4 (a)

627 Fractional Emssivity comparisons between HIRS longwave and shortwave C02 channels. Constraint: from C02 slicing method only.

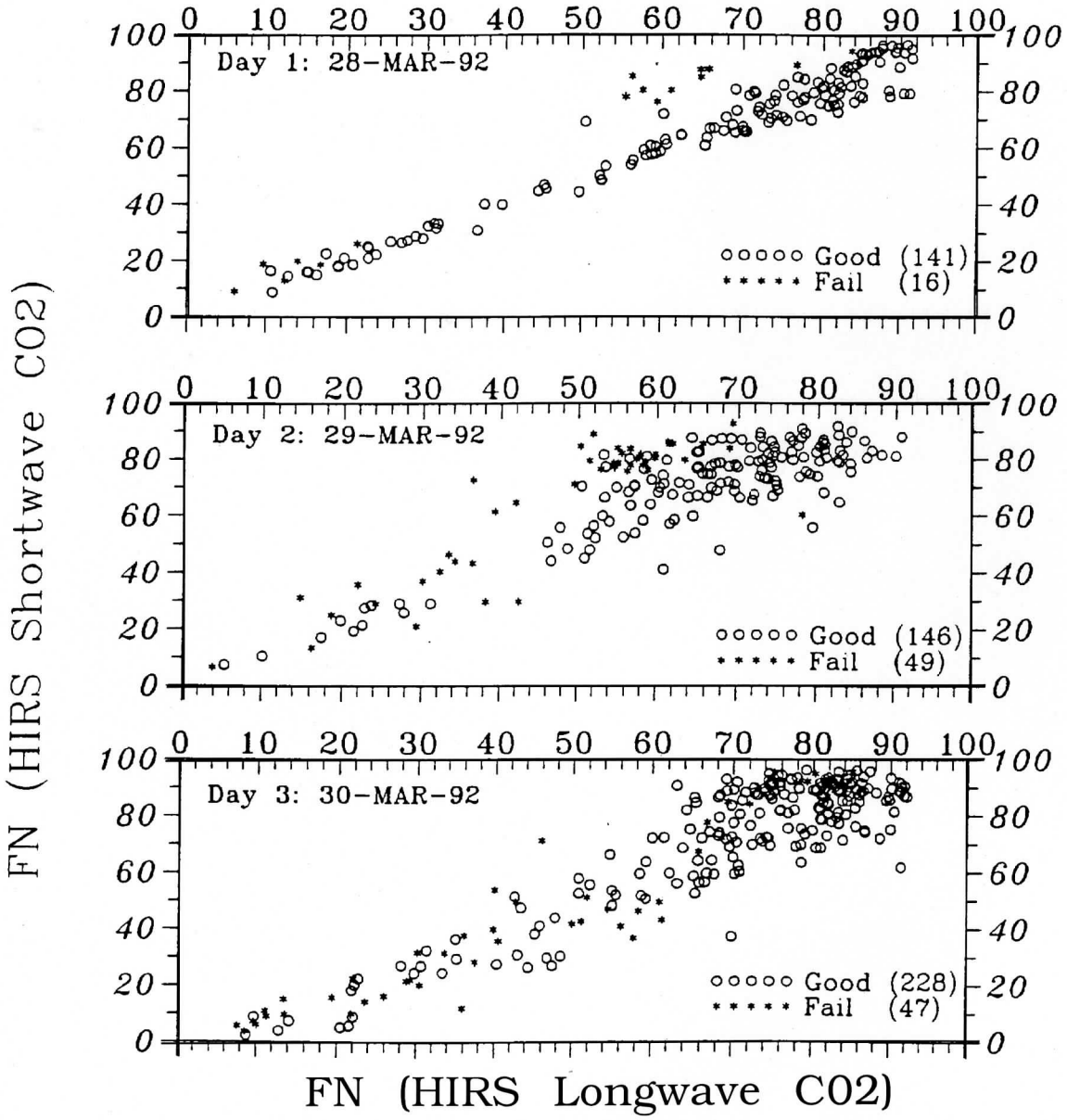

627 Cloud top heights comparisons between HIRS longwave and shortwave C02 channels. Constraint: from C02 slicing method only.

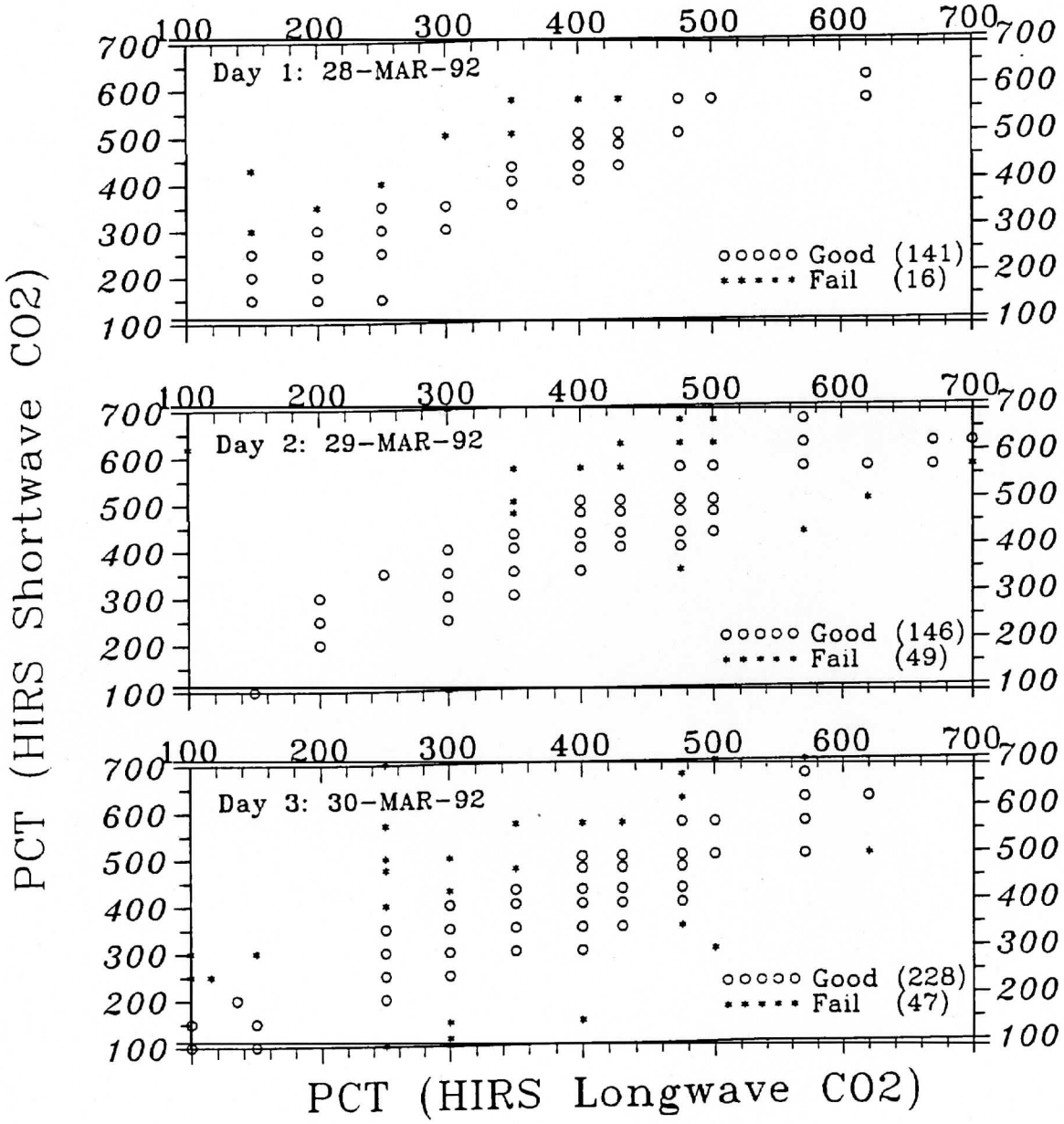

Figure 5

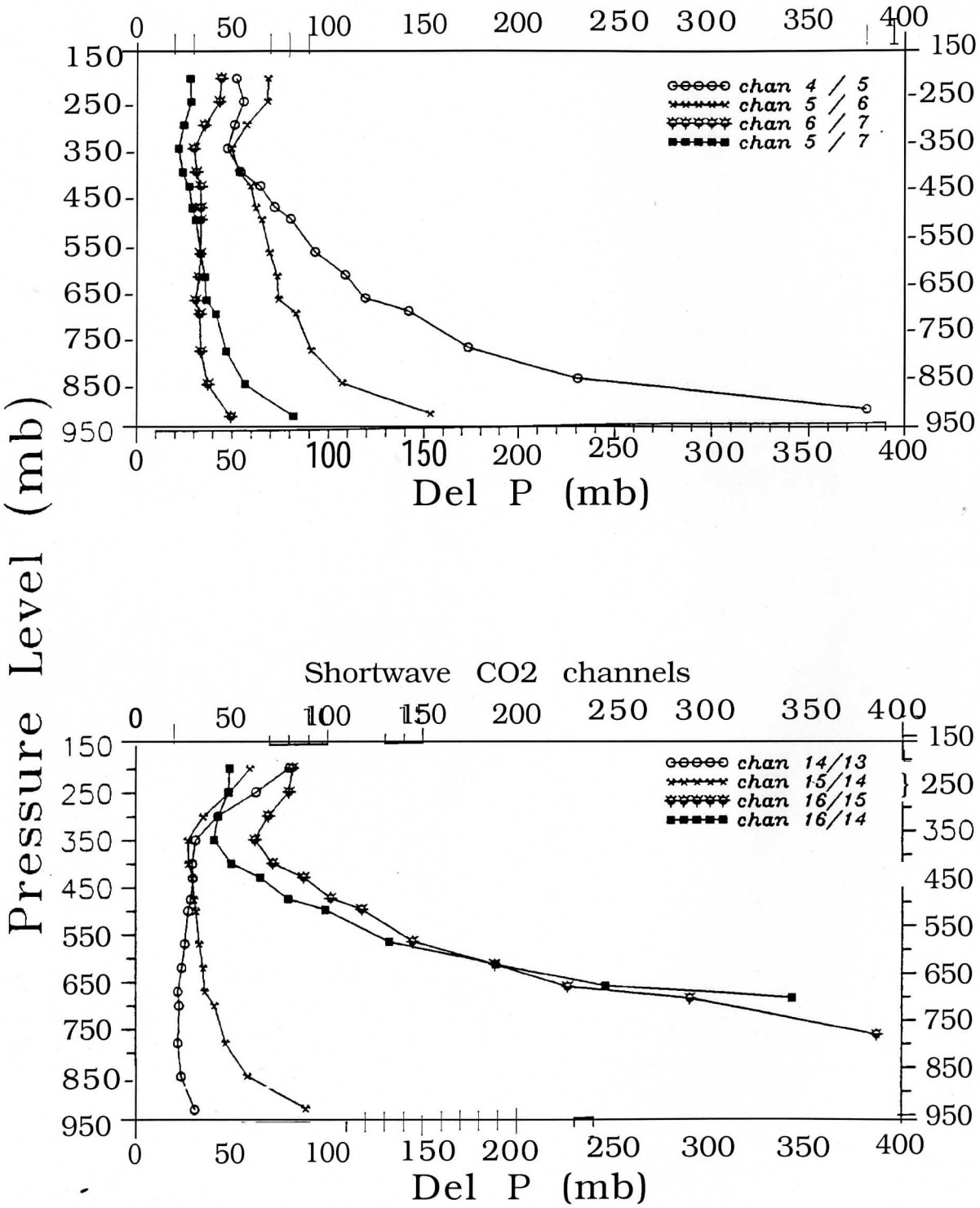
Del P as function of Cloud Top Pressure
Longwave CO2 channels
chan 4 / 5
chan 5 / 6
chan 6 / 7
chan 5 / 7
Shortwave CO2 channels
chan 14/13
chan 15/14
chan 16/15
chan 16/14
Pressure Level (mb)
Del P (mb)
0 50 100 150 200 250 300 350 400
150 250 350 450 550 650 750 850 950

Figure 6

627 Fractional Emssivity comparisons between HIRS longwave and shortwave C02 channels. Constraint: from C02 slicing method only.

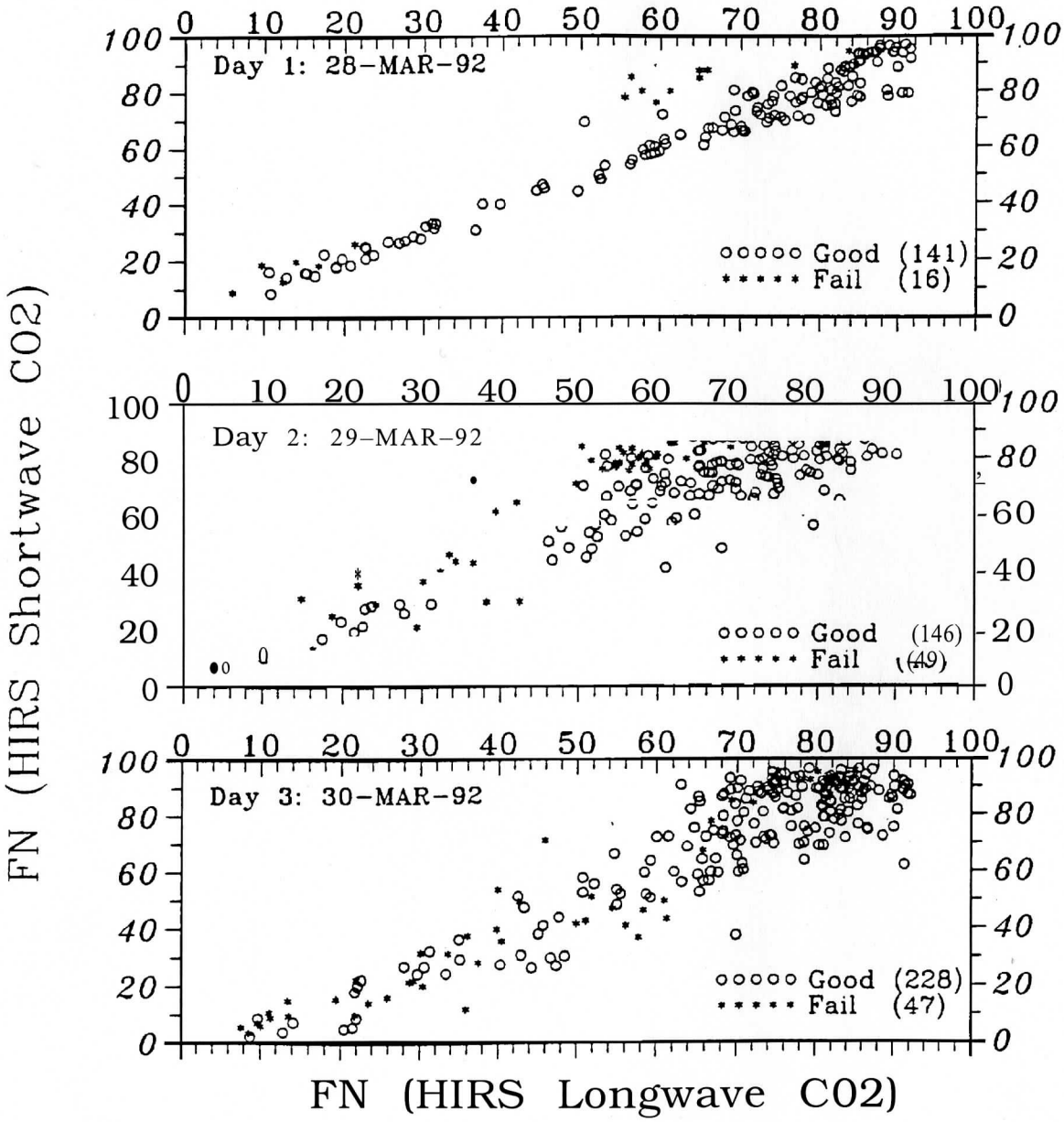

Figure 7